Deformation and fracture mechanisms of selective laser melted tungsten skeleton reinforced copper matrix composites at varied temperatures

Rong Li[1], Wenge Chen[1*], Kai Zhou[1], Yana Yang[1], Longlong Dong,[2] Ahmed Elmarakbi[3], Yong-Qing Fu[3*]

1 School of Materials Science and Engineering, Xi'an University of Technology, Xi'an, Shaanxi, 710048, P.R. China

2 Advanced Materials Research Central, Northwest Institute for Nonferrous Metal Research, Xi'an 710016, PR China

3 Faculty of Engineering and Environment, Northumbria University, Newcastle upon Tyne, NE1 8ST, UK.

Abstract: Tungsten skeleton reinforced copper matrix composites (TRC) were designed and fabricated using a selective laser melting (SLM) method followed by infiltration sintering. Deformation and fracture mechanisms were investigated at 25, 300 and 500 ºC. Compressive and tensile tests of the tungsten skeletons showed brittle fracture mode, whereas tensile tests of the TRC exhibited a mixed mode of ductile and brittle fracture. Fracture mechanisms of the TRC were identified as cleavage of tungsten and separation between copper and tungsten at 25 ºC. Whereas at 300 and 500 ºC, its fracture mechanisms were identified as intergranular fracture of tungsten particles, tearing of copper and separation between copper and tungsten.

Keywords: Additive manufacturing, porous materials, metallic composites, deformation and fracture

1 Introduction

Copper matrix composites with good conductivities and mechanical properties are promising for applications such as plasma-facing heat-sink materials, guides for electromagnetic railguns, and electrical contacts [1]. For these applications, the copper matrix composites are often reinforced by refractory metals such as tungsten. Copper-tungsten (Cu-W) composites are usually prepared using powder metallurgy due to mutual insolubility and significantly differences in melting temperatures of tungsten and copper. However, it is difficult to prepare Cu-W composites with a high copper

[1] Corresponding authors: Professor Wenge Chen; Prof. Richard Y.Q.Fu.
E-mail: wgchen001@263.net (W.G. Chen), richard.fu@northumbria.ac.uk (Richard Y.Q. Fu)

content (e.g., >50wt.%) through conventional method because tungsten tends to become aggregated resulting in inhomogeneous microstructures of composites [2]. Additive manufacturing (AM) has been used to produce refractory metals [3] and Cu-W composites [4]. So far, tungsten skeletons with a porosity over 80% [5] have been achieved by SLM. Also, Cu-W composites have been fabricated using various additive manufacturing methods [6].

Although there are many studies about the effects of printing paraments on microstructure and mechanical properties, little studies have been done about Cu-W composites with a high copper content and mechanical properties at high temperatures which are important for practical applications. In this study, we designed and fabricated tungsten skeleton and TRC using the SLM method followed by infiltration sintering. Mechanical behaviors and fracture mechanisms of the tungsten skeleton and TRC were studied at varied temperatures (e.g., 25 °C, 300 °C and 500 °C).

2 Experimental

Tungsten powder (30 μm, 99.9%) and copper powder (40 μm, 99.9% purity) were used as the raw materials. Tungsten skeleton with a cubic unit (with a theoretical porosity of 90%) was designed using SolidWorks, and the structure is illustrated in Fig. 1(a). An SLM equipment (EOS-M209) was used to print out the tungsten skeleton specimens with argon as the carrier gas. The laser power, scanning speed, scan interval and layer thickness were 300 W, 450 mm/s, 60 μm, 25 μm. A tube furnace (GSL1700) was used for infiltration and sintering processes, using nitrogen as the protective gas. The furnace was heated up to 1300 °C and maintained for 90 min. Finally, the furnace was naturally cooled down to room temperature to form the TRC.

Morphology of the samples were characterized using an optical microscope (Leica Q2). Porosities and relative densities of samples were measured using Archimedes principle. Crystalline structures of samples were identified using an X-ray diffractometer (XRD, Shimadzu-7000S). Room temperature compressive tests were performed using an HT-2402 computerized servo-controlled material tester according to standard T31930-2015, China. The compression specimens had a dimension of 10 × 10 × 10 mm. Room and high temperature tensile tests were performed using the CMT5105 and DDL50 electronic universal testing machine according to standard T228.1-2010, China. The tensile specimens had a dimension of 20 × 4 × 2 mm. Three samples were measured for the compression and tensile tests with a loading rate of 0.5

mm/min. Fracture surfaces were characterized using a scanning electron microscope (SEM, JEOL JSM-6700F) equipped with an energy dispersive X-ray spectroscope (EDS).

3 Results and discussion

Figs. 1(c) shows a photograph of the printed tungsten skeleton. The measured porosity of tungsten is 85.50±2.60%, lower than that of theoretical value result from several reasons. During the SLM process, firstly, formation of overhang microstructures under the horizontal struts and partially un-melted particles on the struts surfaces resulted in the decrease of pore sizes. [7]. Secondly, there are some pores formed within the struts during melting and solidification processes due to high temperature gradients generated [8], which result in the increased thickness of struts and decreased porosity. Finally, the errors in the measurement processes partially contribute to the differences between the actual and theoretical value. Fig. 1(d) shows photograph of the TRC, and the measured relative density is 97.78%. Fig. 1(e) shows the XRD patterns of tungsten powders, tungsten skeleton and TRC. Results show that the tungsten skeleton is consisted of tungsten phases. Furthermore, the amplitude of the tungsten peak in the skeleton sample is significantly increased compared with that of the tungsten powder, which reveals that the tungsten structures become denser and crystals have grown during the SLM process [9]. In addition, the main peaks of tungsten and copper phases are all observed in the TRC without forming any apparent intermediate phases because tungsten and copper are mutually insoluble [10].

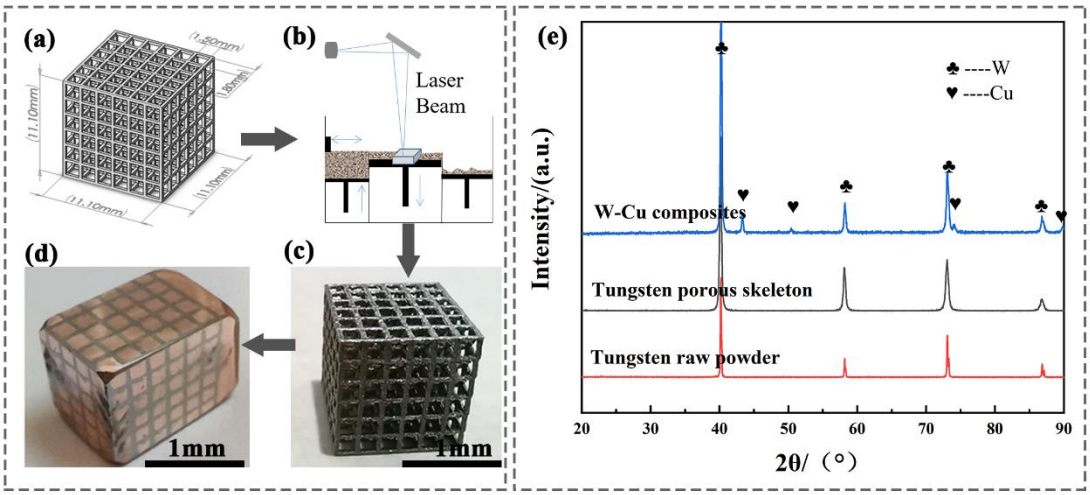

Fig. 1(a) Designed structures of tungsten skeleton; (b) schematic diagram of SLM process; (c) photograph of printed tungsten skeleton and (d) TRC; (e) XRD patterns of tungsten powder, tungsten skeleton and TRC

Figs. 2(a1) and 2(a2) show the representative stress-strain curves of tungsten skeleton under compressive and tensile deformation. The calculated compressive and tensile strengths are ~22±2.90 MPa and ~36±3.50 MPa. The two curves consist of an initial linear-elastic region, followed by a dramatically reduced stress value, which shows a typical brittle fracture mode. Figs. 2(b1) and 2(b2) show fracture morphologies of compression tests. It is obvious that un-melted particles of tungsten (see Fig. 2(b1)) in the sintered structures are responsible for its early fracture [5]. Also, the large values of waviness and roughness for the struts cause the increased local stress concentrations, thus leading to a lower compressive strength [11]. Fig. 2(b2) presents a typical brittle fracture feature with distinctive cleavage steps and facets. Similarly, obvious cleavage steps and facets can be observed from Figs. 2(c1) and 2(c2). It was reported in Ref. [12] that the large residual stresses were generated in joint of struts during the SLM process due to significantly large cooling rates and shrinkages after melting. Consequently, cracks are generated at the local stress concentration sites and easily propagate under the continuously increased stress. Finally, tungsten skeletons were fractured with a typical brittle fracture mode for both compressive and tensile tests.

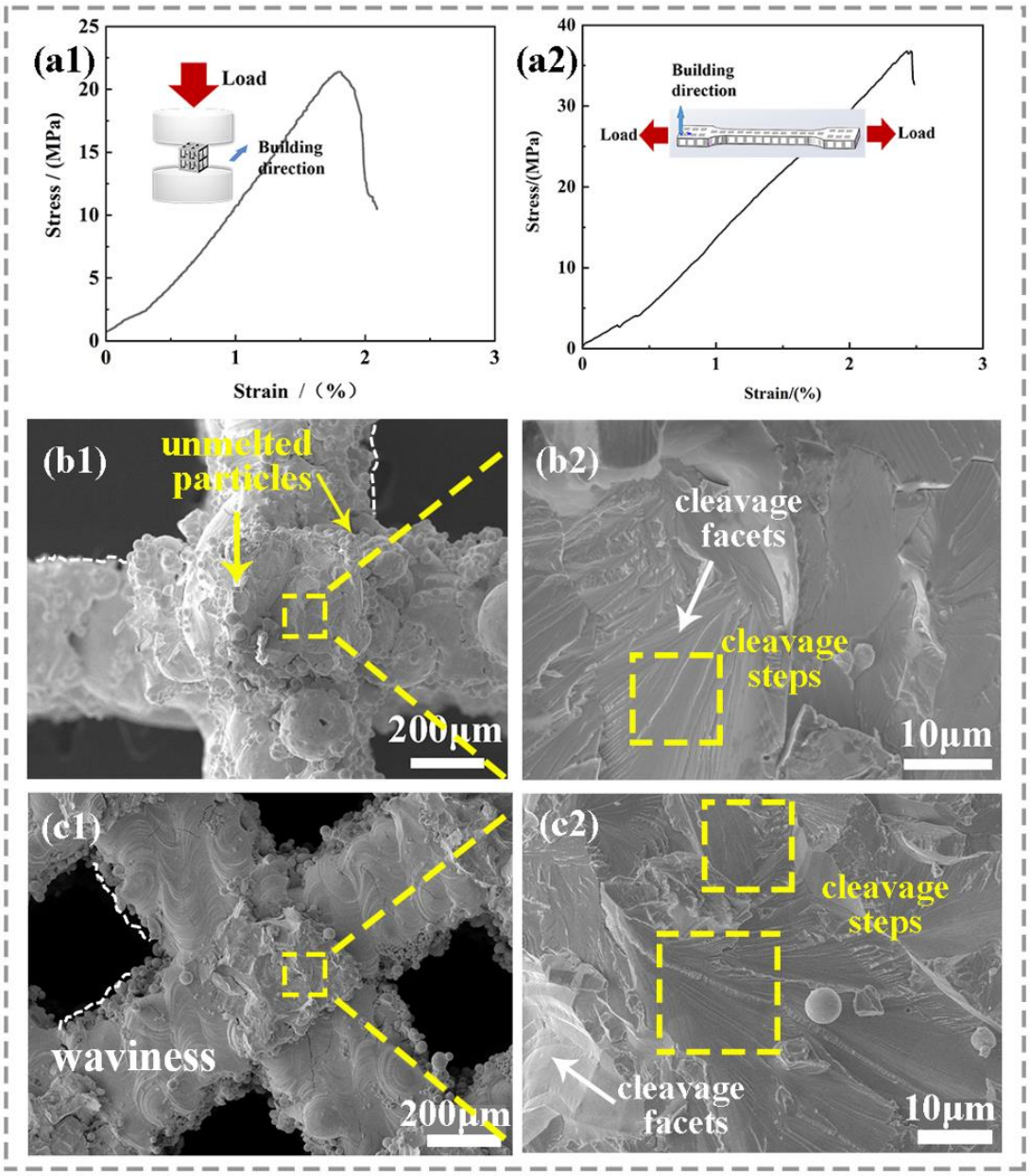

Fig. 2(a1) Compressive and (a2) tensile stress-strain curves of tungsten skeleton; (b1) and (b2) fracture morphologies under compression; (c1) and (c2) under tensile process

Fig. 3(a1) shows the typical tensile stress-strain curves of TRC at 25, 300 and 500 °C. Elastic and plastic deformation behaviors have been observed for all the samples. The slopes of the straight lines during the elastic deformation stage at 300 and 500 °C are smaller than those tested at 25 °C, which is attributed to the softening of materials at a high temperature. The calculated tensile strengths are 103, 98 and 59 MPa, and the corresponding elongations at break are 20.9, 19.1 and 17.2 (Fig. 3(a2)), which may be related to the initiation of cracks in weaker interfaces of tungsten and copper, thus weakening the softening effect. The tensile strength for TRC reached ~103 MPa at room temperature, which is approximately 110% higher than that of the pure copper.

Figs. 3(b1~b4), 3(c1~c4) and 4(d1~d4) are SEM images of the fracture morphologies tested at 25, 300 and 500 °C, respectively. The fracture images shown in Figs. 3(b1), 3(c1) and 3(d1) display smooth surfaces of the tungsten and uneven surfaces of the copper at different temperatures. The tensile sample shows mixed-modes of plastic and brittle fracture. At 25 °C, the cleavage steps and facets are observed as shown in Fig. 3(b2), which are the typical brittle fracture features. Some torn edges can be observed as shown in Fig. 3(b3), indicating certain degree of ductility. When tested at 300 °C, the fracture surface shows intergranular fracture features as shown in Fig. 3(c2) and many small dimples can be observed in Fig. 3(c3). When tested at 500°C, the fracture surface shows some fibrous structures (see Fig. 3(d2)), and the copper also shows dimples and oxidized features (see EDX inset in Fig. 3(d3)).

The fracture mechanisms of TRC at different temperature are summarized as follows. At 25 °C, the interconnected copper and tungsten are successively subjected to stress, so the curve shows a typical jagged feature (see Fig. 3(a)). The residual micro-pores in the struts and gaps between copper and tungsten tend to create large stress concentration under further straining stress and then cause crack initiation and propagation. Therefore, the fracture mechanisms are cleavage of tungsten and separation between copper and tungsten. At 300 °C, the difference in the thermal expansion coefficient leads to large stress concentration at the interfaces of copper and tungsten, which promotes more crack generation. While the copper shows the ductile deformation behavior. At 500 °C, the oxidation of copper phase weakens the interfacial bond strength between copper and tungsten, thus causing the further initiation and propagation of cracks. Consequently, at higher temperatures, cracks are mainly initiate at the weak interfaces between copper and tungsten, and then propagate along the interfaces. Finally, the sample breaks up under the increased stress. The fracture mechanisms are intergranular fracture of tungsten particles, tearing of copper and separation between copper and tungsten.

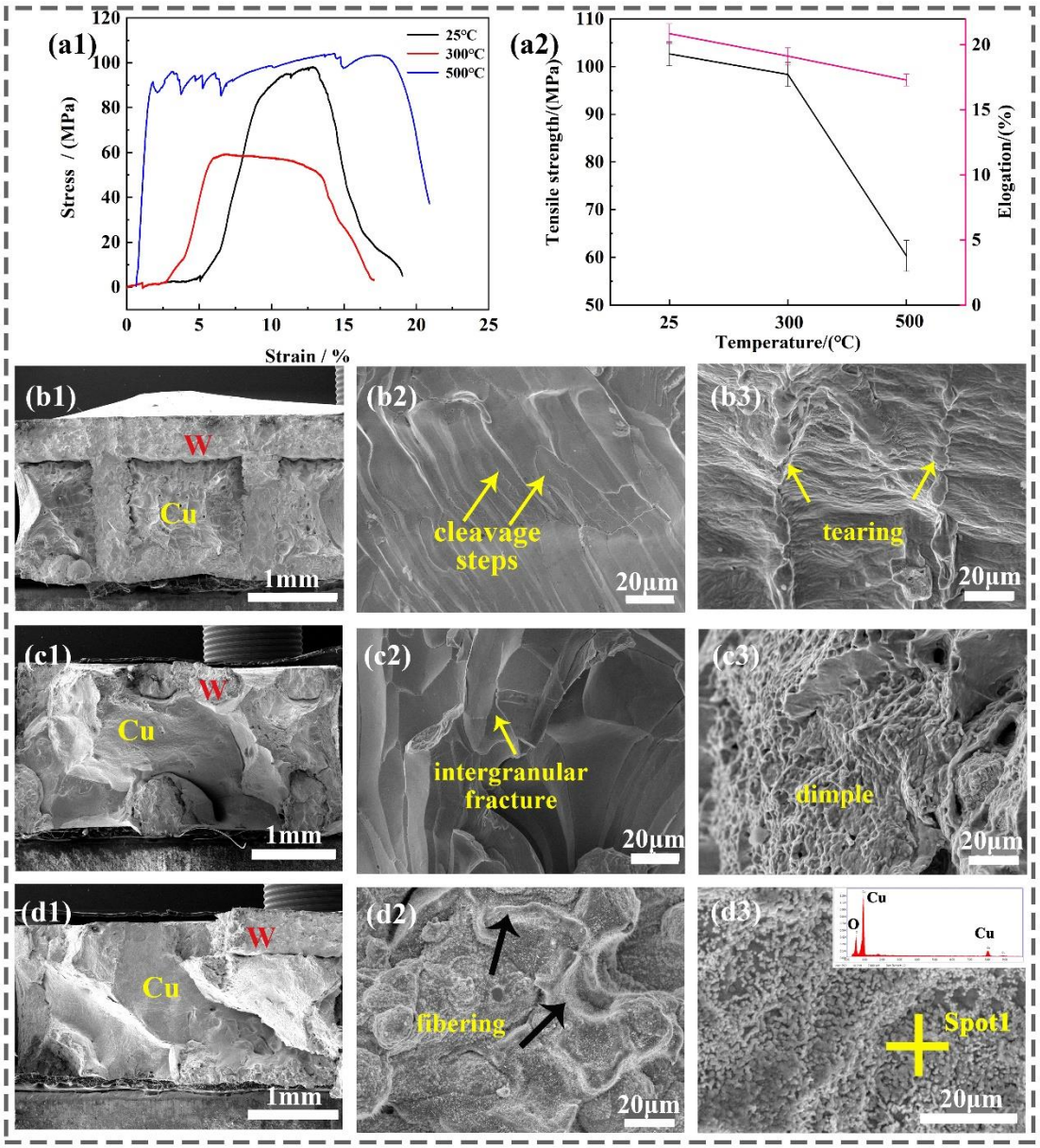

Fig. 3(a1) Tensile stress-strain curves of TRC; (a2) variation of tensile strength and elongation with temperature; fracture morphologies (b1~b3) at 25 °C, (c1 ~ c3) at 300 °C, (d1 ~ d3) at 500 °C; (b2), (c2) and (d2) further magnification of tungsten phases; (b3), (c3) and (d3) further magnification of copper phases

4 Conclusion

The tungsten skeleton prepared by the SLM displays brittle cleavage fracture modes in both compression and tensile tests, and the compressive and tensile strength are 22 MPa and 36 MPa, respectively. With the increased testing temperature, the strength of the TRC is decreased from 103 MPa to 59 MPa, and the elongation is decreased from 20.9% to 17.2%. When tested at 25 °C, the TRC shows fracture

mechanisms of tungsten cleavage and separation between copper and tungsten. Whereas at 300 and 500 °C, the fracture mechanisms become intergranular fracture of tungsten particles, tearing of copper and separation between copper and tungsten.

Acknowledgments

The authors would like to acknowledge the financial supports from National Natural Science Foundation of China (No. 51901192), Key Research and Development Projects of Shaanxi Province (No. 2020ZDLGY12-06), National Program for Introduction of Foreign Experts (G2022041019L) and International Exchange Grant IEC/NSFC/201078) through Royal Society and National Science Foundation of China.

References

[1] Q. Lin, B. Li, et al. Def. Tech. 2020,16(02):348-353.
[2] S. Liang, L. Chen, et al. Mater. Des. 2015, 110:33-38.
[3] D. Faidel, D. Jonas, et al. Addit. Manuf. 2015, 8:88-94.
[4] A. Ivekovic, N. Omidvari, et al. J. Refract. Met. Hard Mater. 2018.
[5] K. Zhou, W. Chen, et al. J. Refract. Met. Hard Mater. 2021.
[6] D. Zhang, C. Kenel, et al. Acta Mater. 2021.
[7] Ran Q, Yang W, Hu Y, et al. J Mech Behav Biomed. 2018, 84: 1-11.
[8] Thijs L, Verhaeghe F, et al. Acta Mater 2010;58:3303–12.
[9] X. Ren, H. Liu, F. Lu, et al. J. Refract. Met. Hard Mater. 96. 2021.105490.
[10] A. Yan, Z. Wang, et al. Mater. Des. 2016. 07.049.
[11] Van Bael, S., Kerckhofs, et al. Mater. Sci. Eng. A. 2011.528,7423–7431.
[12] J. Sun, Y. Yang, et. al. Mater. Des. 2013.01.038.